Journal of Marine Research, 42, 809–829, 1984

On the equatorial Pacific response to the 1982/1983 El Nino—Southern Oscillation event

by T. Y. Tang[1,2] and R. H. Weisberg[1,2]

ABSTRACT

The ocean's response to the 1982/83 El Nino—Southern Oscillation event was the largest ever documented. In this paper we explore the effects of certain details of the observed zonal wind stress anomaly field upon the ocean's response using a linear, adiabatic, reduced gravity, analytical model. The increase in magnitude of the downwelling response over the composite of previous El Nino events is attributed to the eastward translation of the observed westerly wind anomaly and the double peaked downwelling at the South American coast is attributed to the amplitude modulation of this anomaly. Effects of an easterly anomaly which appeared to the west of the dateline midway through the event are also considered.

1. Introduction

Roughly twice per decade the eastern half of the equatorial Pacific Ocean is visited by diminished tradewinds and elevated sea surface temperature (SST) and rainfall. As discussed by Horel and Wallace (1981), these El Nino—Southern Oscillation events have global climatic consequences. Rasmusson and Carpenter (1982) constructed a composite El Nino event based upon six such occurrences since 1949. Preceding the composite event the equatorial easterlies are stronger than normal to the west of the dateline. These easterly wind anomalies reverse to become westerly anomalies after which anomalously warm SST appears in the eastern equatorial Pacific. Conditions return to normal after around one year. Philander (1983) reviews theory, observations, and questions regarding the El Nino—Southern Oscillation.

A major El Nino event occurred during 1982/83 which differed in several aspects from the historical composite. As shown by Rasmusson *et al.* (1983) and Rasmusson and Wallace (1983), the westerly wind anomaly differed in that it migrated eastward across the Pacific Ocean and the SST anomaly differed in that its indices were twice as large as the composite and it exhibited a double peak; the first one over the eastern half of the equatorial Pacific followed by an even larger second peak at the South American coast.

1. Department of Marine, Earth and Atmospheric Sciences, North Carolina State University, Raleigh, North Carolina, 27650, U.S.A.

2. Present address: Department of Marine Science, University of South Florida, 140 Seventh Avenue South, St. Petersburg, Florida, 33701, U.S.A.

The purpose of this paper is to illustrate the connection between the manner in which the wind anomalies progressed during the 1982/83 event and the unprecedented nature of the ocean's response.

The paper will proceed as follows. Section 2 will review the observations and previous modelling studies germane to our results. Analytical procedures are described in Section 3. Section 4 compares results for westerly wind anomalies that are stationary, translatory, and translatory with varying amplitude. By comparing responses to stationary and translatory westerly anomalies with equal fetch and amplitude under Case A, we demonstrate the effect of significantly increased downwelling caused by the eastward translation. By varying the amplitude of the westerly anomaly as it translates in Case B, we produce the second downwelling peak observed at the South American coast. The results are discussed in Section 5 where the effects of an easterly anomaly that appeared to the west of the dateline midway through the 1982/83 event are added. Finally Section 6 provides a summary.

2. Background

Figure 1 from Rasmusson *et al.* (1983) shows the 850 mb zonal wind velocity component and SST anomalies as functions of longitude and time. Beginning around June 1982 we observe a westerly wind anomaly forming to the west of the dateline. The amplitude of the anomaly intensifies and then remains constant through around Oct. 1982. It then decreases and increases again to a second maximum around Feb. 1983, after which it subsides. As the amplitude varies the anomaly progresses steadily eastward at a rate of around 0.5 m/s. Associated with the local minimum is the establishment of an easterly anomaly to the west of the dateline and associated with the second maximum is an increased fetch. Positive SST anomaly peaks in the interior portion of the eastern equatorial Pacific around Dec. 1982. Although its maximum is centered between 120W–140W, the anomaly extends over one quarter of the earth's equatorial circumference. The SST anomaly interior to the basin subsides after Jan. 1983 but an even larger second maximum appears on the eastern boundary between April–June 1983. Rasmusson *et al.* (1983) showed that the index of the 1982/83 SST anomaly interior to the basin (an areal average from 90W–150W between $\pm 5°$ of the equator) was more than twice that of the Rasmusson and Carpenter (1982) composite El Nino anomaly and that the second peak at the coast was substantially more pronounced.

Velocity and temperature data from Halpern (1983) collected on the equator at 110W are shown in Figure 2. Departures from the seasonal cycle are clearly evident during July 1982 when temperatures at all levels sampled (15 m–100 m) begin to rise. Taking 100 m as being indicative of the thermocline we see a rapid downwelling through Oct. 1982 which continues at a reduced rate to a peak in Dec. 1982. Following the downwelling peak an even more rapid upwelling returns the thermocline to a near normal level. Simultaneous with the thermocline displacement, the upper ocean zonal

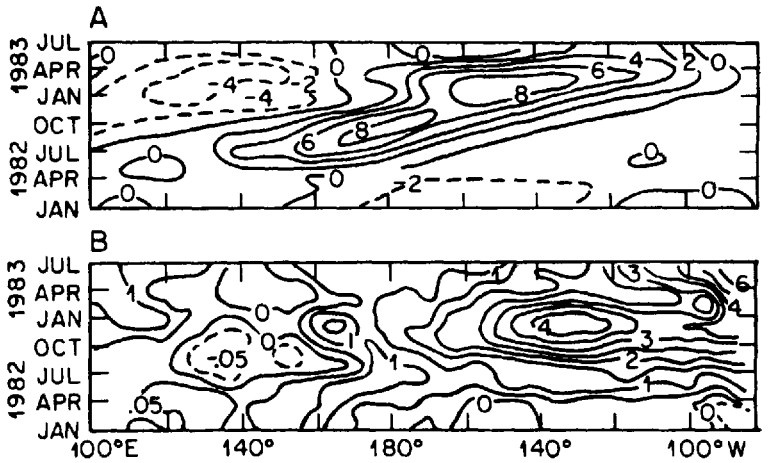

Figure 1. (A) 850 mb zonal wind velocity component anomaly (m/sec) between 5N–5S as a function of longitude and time. Positive values represent westerly anomaly and negative values represent easterly anomaly. (B) SST anomaly (°C) between 5N–5S as a function of longitude and time (from Rasmusson *et al.*, 1983).

velocity component undergoes a sinusoidal oscillation with an initially eastward tendency followed by a westward one and then an eastward one.

There have been numerous modelling efforts aimed at understanding the ocean's response to the anomalous winds accompanying El-Nino events. Adiabatic responses to the relaxation of easterly winds were studied by McCreary (1976) and Hurlburt *et al.* (1976) using reduced gravity models and by Philander (1981) using a multilevel

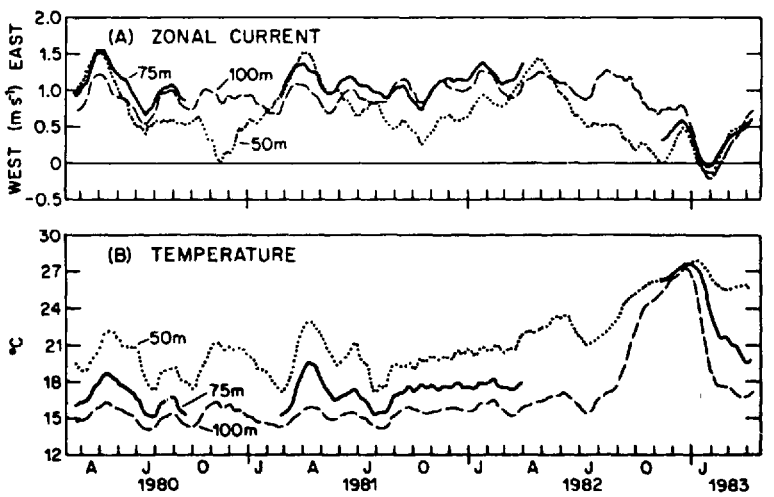

Figure 2. Low pass filtered (A) zonal velocity component and (B) temperature variations observed on the equator at 110W using moored current meters (from Halpern, 1983).

numerical model. Kelvin and long Rossby waves were identified as the principal vehicles for adjusting the pressure field in these models. Busalacchi and O'Brien (1981) and Busalacchi *et al.* (1983) presented simulations of the thermocline variability along the equatorial Pacific from 1960 to 1970 and 1971 to 1978 respectively, periods which encompassed 5 El Nino events, by driving a reduced gravity model with historically derived monthly wind fields. The results, compared with sea level and SST data from island stations and Peru, led these authors to conclude that linear equatorial waves can be used to explain the phase of the ocean response to zonal wind stress variability in the central and western portions of the Pacific Ocean.

It is within the context of adiabatic linear models that we will proceed in an attempt to show that certain details of the 1982/83 zonal wind anomalies can account for the unusually large and double peaked ocean response. Weisberg and Tang (1983) considered westward translating easterly winds with application to seasonal variations in the equatorial Atlantic Ocean. Westward translation increased (decreased) the Rossby (Kelvin) wave responses over those for a stationary wind patch. Reversing the direction of translation to favor the Kelvin wave response is therefore a natural extension of this previous study. Eastward translating zonal wind anomalies also appear in papers by Philander (1983) and Gill and Rasmusson (1983), both of which are primarily concerned with oceanic-atmospheric interaction during an El Nino—Southern Oscillation event.

3. Analytical techniques

Consider a one active layer reduced gravity model on a meridionally bounded equatorial β-plane, nondimensionalized by a horizontal length scale $L_R = (g'H_0)^{1/4}/\beta^{1/2}$ and a time scale $T = (g'H_0)^{-1/4}\beta^{-1/2}$, where g' is the reduced gravity and H_0 is the mean thermocline depth. The equations of motion describing perturbations about a basic state of rest are:

$$\frac{\partial u}{\partial t} - yv + \frac{\partial h}{\partial x} = \tau \tag{1}$$

$$\frac{\partial v}{\partial t} + yu + \frac{\partial h}{\partial y} = 0 \tag{2}$$

$$\frac{\partial h}{\partial t} + \frac{\partial u}{\partial x} + \frac{\partial v}{\partial y} = 0 \tag{3}$$

where x, y and t are the zonal, meridional, and temporal coordinates; u, v, and h are the zonal and meridional velocity components and upper layer thickness perturbations respectively; and τ is the zonal forcing function prescribed as a body force in the upper layer. Cane and Sarachik (1976) discussed the ocean interior solution to the linear forced equatorial wave problem and their techniques are directly applicable here. The

forcing function is first Fourier transformed in x and then projected onto the free equatorial wave modes which form a complete orthogonal set over the interval between $y = \pm\infty$. The coefficients of the forced equatorial wave response are calculated from the forcing function coefficients by integrating over time beginning with the initial conditions $u = v = h = 0$ at $t = 0$. The resulting Fourier transforms are then inverted to obtain the solutions in real space. A long wave approximation for Rossby waves is made in this latter step yielding a solution consisting entirely of nondispersive waves.

Since the solutions are in terms of the free equatorial wave modes a brief review of them is now offered. The homogeneous equations (1)–(3), with dependent variables proportional to exp $\{i(kx-\omega t)\}$, where k and ω are the zonal wavenumber component and frequency respectively, may be reduced to a single equation in v:

$$\frac{d^2v}{dy^2} + (\omega^2 - k^2 - k/\omega - y^2)v = 0. \tag{4}$$

The dispersion relation

$$\omega^2 - k^2 - k/\omega = 2n + 1 \tag{5}$$

results from the boundary conditions that v approaches zero as y approaches $\pm\infty$, and the corresponding eigenfunctions are:

$$v_n(y) = \psi_n(y) = (2^n n! \sqrt{\pi})^{-1/2} e^{-y^2/2} H_n(y), \tag{6}$$

where $n \geq 1$ is an integer meridional mode number and $H_n(y)$ are the Hermite Polynomials (e.g. Matsuno, 1966). Two additional special solutions exist: the Kelvin wave ($n = -1$) for which $\omega = k$ and v is identically zero, and the Rossby-gravity wave ($n = 0$) for which $\omega - 1/\omega = k$. For $n \geq 1$, the waves are either Rossby waves or inertia-gravity waves. The former are quasi-geostrophic low frequency waves whose dispersion relation simplifies in the long wave limit to $\omega = -k/(2n + 1)$. The latter are ageostrophic high frequency waves.

Forcing functions symmetric about the equator will project only onto even Hermite polynomials. The u and h fields have opposite symmetry from the v field so only odd numbered waves are excited by symmetric zonal forcing. Convergence of the eigenfunction expansion and consequently the number of modes required depends upon the meridional scale of the forcing. Tapering the forcing function to zero away from the equator does not appreciably affect the lowest modes which Cane and Sarachik (1976) showed to be the principal contributors to the response on the equator. For the present calculation we choose a forcing function proportional to $\exp(-y^2/2)$. This has the same form as $\psi_0(y)$ so it projects only onto the Kelvin and first mode Rossby waves which greatly simplifies the overall solution. Quantitative comparisons between Gaussian tapered and meridionally uniform zonal wind stress distributions are given in Weisberg and Tang (1983) for the case of westward moving fetch which favors excitation of Rossby waves. Although tapering increases the Rossby wave relative to

the Kelvin wave projection over that for the meridionally uniform case, the qualitative results for both cases are very similar.

For the present calculation where we will be concerned primarily with a downwelling response, the tapering provides for a conservative simplification since the more complicated meridionally uniform case would result in a relatively larger Kelvin wave response and hence larger downwelling.

The forced interior Kelvin and first Rossby mode solutions reflect upon reaching meridional boundaries. Moore and Philander (1977) and Cane and Sarachik (1977) discussed these reflections in detail. At the western boundary, the incoming mass flux associated with the long Rossby wave integrated between $\pm\infty$ is carried away by a reflected Kelvin wave. At the eastern boundary, the incoming Kelvin wave is reflected as the sum of outgoing long Rossby waves of the same symmetry, i.e., modes 1, 3, 5, etc.

After calculating the forced interior projections and boundary reflections through Rossby wave mode 5, the results are summed to give the total long wave solutions.

4. Results

Case A. Westerly wind anomaly with constant amplitude and fetch either stationary or eastward translating. Here we compare the equatorial thermocline and zonal velocity component responses to a uniform westerly wind anomaly which is either stationary to the west of the dateline or translatory across the Pacific Ocean. The forcing function is:

$$\tau(x, y, t) = \gamma e^{-y^2/2}\{H(x - \alpha t) - H(x - L - \alpha t)\} \tag{7}$$

where the H's are step functions, equaling zero or one for negative and positive arguments respectively, α is the eastward translation speed, γ is the magnitude of the wind stress anomaly, and L is the length of the fetch. The dimensions of the ocean response thus depend upon γ, α, L, and the reduced gravity baroclinic wave speed $(g'H_0)^{1/2}$. In terms of longitude, Figure 1 suggests initial values of L and α to be around 40 degrees and 10 degrees per month respectively. Nava and Ripa (unpublished manuscript) composited an average density profile along the equator from 180W to 110W which gave a reduced gravity wave speed of 2.4 m/s and a similar number was used in the Busalacchi and O'Brien (1981) simulations. Based upon these suggestions the parameters used to explore the forced response of Case A are as follows: $L = 40$ degrees, $\gamma = 0.021$ which corresponds dimensionally to a wind stress of 1 dyne/cm^2, $(g'H_0)^{1/2} = 250$ cm/s, and $\alpha = 50$ cm/sec. Nondimensionally $\alpha = 0.2$.

The interior Kelvin and $n = 1$ Rossby wave solutions are:

$$\begin{aligned} u_k(x, y, t) = h_k(x, y, t) = \frac{\gamma\pi^{1/4}}{2(1 - \alpha)}\psi_0(y)\{&(x - \alpha t)H(x - \alpha t) \\ &-(x - t)H(x - t) - (x - L - \alpha t)H(x - L - \alpha t) \\ &+ (x - L - t)H(x - L - t)\} \end{aligned} \tag{8}$$

and

$$\begin{bmatrix} u_R(x, y, t) \\ h_R(x, y, t) \end{bmatrix} = -\frac{\gamma\pi^{1/4}\sqrt{2}}{4(\alpha + 1/3)} \{(x + t/3)H(x + t/3) - (x - \alpha t)H(x - \alpha t) - (x - L + t/3)H(x - L + t/3) + (x - L - \alpha t)H(x - L - \alpha t)\} \cdot \begin{bmatrix} \frac{-2\sqrt{2}}{3}\psi_0(y) + \frac{2}{3}\psi_2(y) \\ \frac{2\sqrt{2}}{3}\psi_0(y) + \frac{2}{3}\psi_2(y) \end{bmatrix}. \quad (9)$$

Relative to an initially undisturbed thermocline the interior Kelvin and Rossby wave responses give downwelling to the east and upwelling to the west of the forced region respectively. To the east, downwelling will commence at a time $t = x - L$ when the leading edge of the Kelvin wave arrives and will proceed until $t = x$ when the trailing edge of the Kelvin wave arrives. During this interval the downwelling will be proportional to $t/(1 - \alpha)$ since it is an integral response. Thus, the interior downwelling Kelvin wave response for eastward moving fetch will exceed that for fixed fetch by an amount $1/(1 - \alpha)$. Similarly, the interior upwelling Rossby wave response for eastward moving fetch will be reduced from that for fixed fetch by an amount $1/3/(\alpha + 1/3)$. Upon reaching the western boundary the interior upwelling Rossby wave will reflect as an upwelling Kelvin wave which will then propagate eastward. Therefore both the increase of the interior downwelling Kelvin wave and decrease of the interior upwelling Rossby wave give rise to an increased downwelling response for eastward moving fetch over stationary fetch.

Employing the reflection formalisms referenced in Section 3, we arrive at the total long wave solutions summed through the fifth mode reflected Rossby wave. These are shown as a function of longitude and time in Figures 3 and 4 for the upper layer thickness and zonal velocity component perturbations respectively. The model basin is bounded on the west by 130E and on the east by 80W. The wind anomaly of Eq. 7 is switched on at $t = 0$ between the western boundary and 170E which corresponds roughly with July 1982 (Fig. 1). The anomaly then progresses eastward without change in form at a uniform rate of 50 cm/sec ($\alpha = 0.2$). The forced region, the interior and reflected Kelvin wave responses and the reflected Rossby waves are all easily discernable in the contours, the reflected Rossby waves being particularly clear in Figure 4.

By taking a time slice at 110W we can discuss the evolution of the pattern. This is shown in Figure 5 for the upper layer thickness perturbation, the solid line corresponding to the moving wind anomaly and the dashed line corresponding to the stationary wind anomaly. Consider the solid line first. No response is evident until the leading edge of the interior Kelvin wave arrives. Downwelling then proceeds until the trailing edge arrives. This time also coincides with the arrival of the leading edge of the

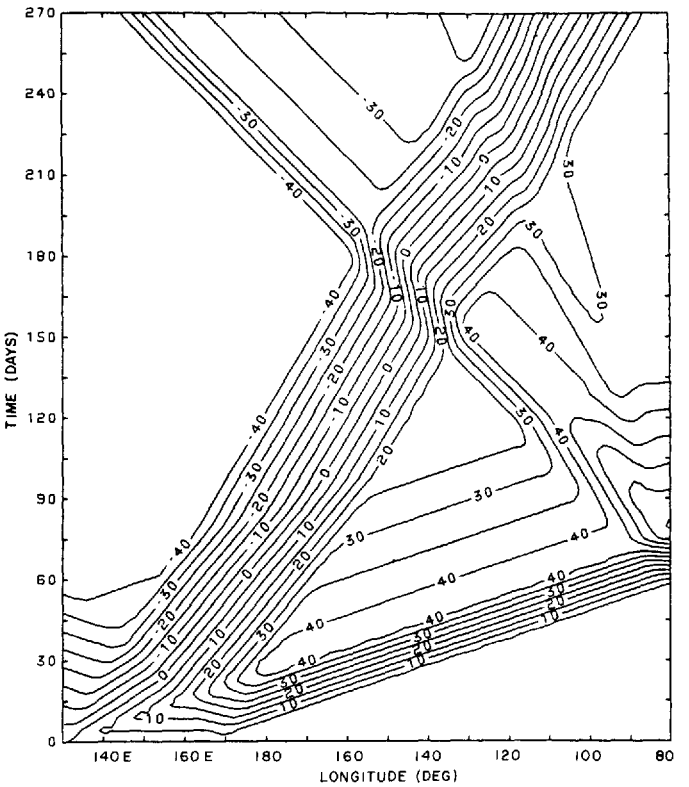

Figure 3. Upper layer thickness perturbation, h, evaluated on the equator as a function of longitude and time for a westerly wind stress anomaly of constant amplitude (1 dyne/cm^2) and fetch (40°) which translates eastward at a rate α = 50 cm/sec relative to a reduced gravity wave phase speed of $(g'H_0)^{1/2}$ = 250 cm/sec. The contour interval = 5 m.

upwelling Kelvin wave originating at the western boundary as a reflection of the interior Rossby wave response. Each change in slope thereafter is attributed to the arrival and subsequent passage of the reflected Rossby waves generated at the eastern boundary and the eventual arrival of the forced region itself. Note that all reflected Rossby waves come in downwelling/upwelling pairs since they originate from a downwelling/upwelling Kelvin wave pair. Now consider the dashed line corresponding to stationary fetch. The interior Kelvin wave response grows at a rate 0.8 times slower than the solid line and the reflected Kelvin wave (originating from the interior Rossby wave response) decreases the downwelling at a rate 1.6 times faster than the solid line. This downwelling favorable state then continues through all of the subsequent reflected Rossby waves. The end result is a substantially larger and longer lived downwelling at 110W for the eastward translating westerly wind stress anomaly over that for a stationary anomaly. In fact, in this simplification, the downwelling associated with eastward translating fetch does not subside until the fetch actually

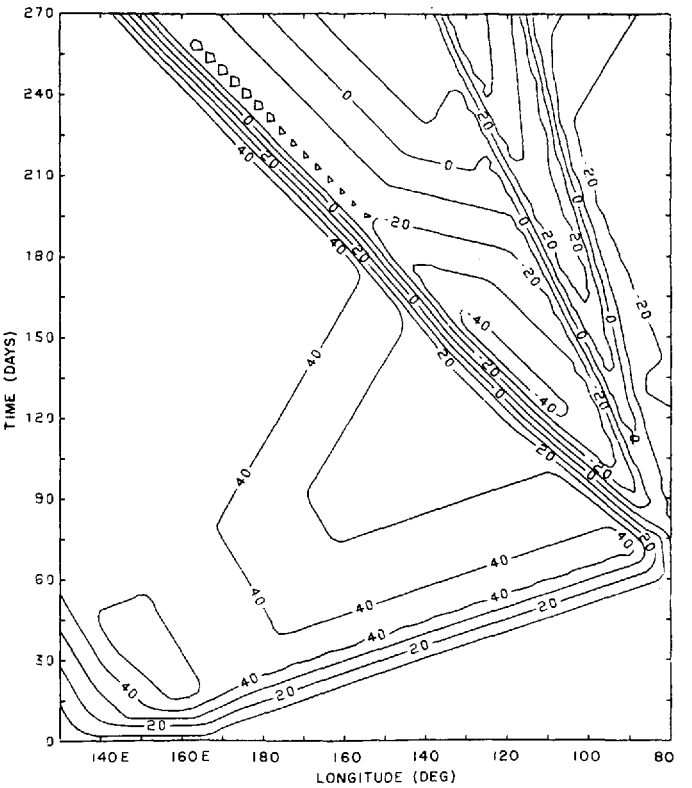

Figure 4. Upper layer zonal velocity component perturbation, u, evaluated on the equator as a function of longitude and time for a westerly wind stress anomaly of constant amplitude (1 dyne/cm^2) and fetch (40°) which translates eastward at a rate α = 50 cm/sec relative to a reduced gravity wave phase speed of $(g'H_0)^{1/2}$ = 250 cm/sec. The contour interval = 10 cm/sec.

reaches 110W, a result which is artificial since Figure 1 suggests that the fetch did not pass beyond 110W.

The evolution of the zonal velocity component perturbation at 110W is shown in Figure 6. Substantial differences between the stationary and translating fetch anomalies are not observed since unlike the upper layer thickness, the zonal velocity component phase difference between incident and principal reflected wave is π radians. Consider the solid line corresponding to translating fetch. It is helpful to view the variations as pairs. The first pair consists of the eastward accelerating interior Kelvin wave response followed by the westward accelerating western boundary reflected Kelvin wave response. Next come the westward and subsequent eastward acceleration of first mode Rossby wave reflections of the Kelvin wave pair at the eastern boundary followed by the third and fifth mode Rossby wave pairs. The net result is a nearly sinusoidal variation in the zonal velocity component.

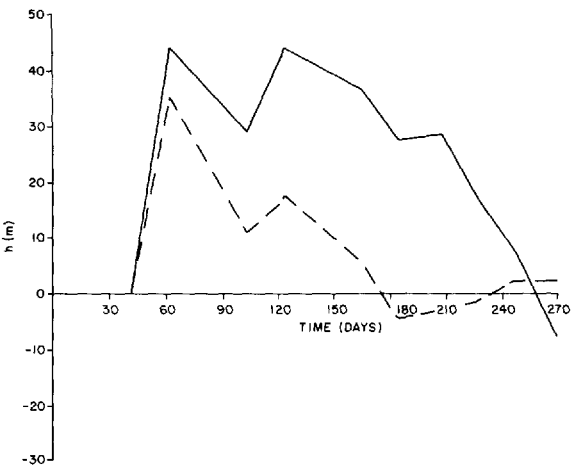

Figure 5. Upper layer thickness perturbation, h, as a function of time evaluated on the equator at 110W for Case A. The result for eastward translating fetch (solid line) is compared with that for stationary fetch (dashed line).

Case B. Eastward translating westerly wind stress anomaly with varying amplitude. As observed in Figure 2, the downwelling peak reached in Dec. 1982 is immediately followed by an even more rapid upwelling. This coincides with a decrease in the SST anomaly over a broad expanse of the eastern equatorial Pacific as seen in Figure 1. Following the decrease in SST anomaly over the interior ocean a sharp secondary SST anomaly appears off the South American coast during May and June 1983. To

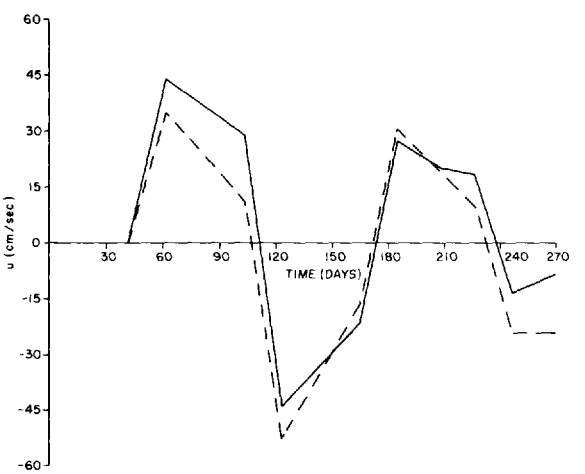

Figure 6. Upper layer zonal velocity component perturbation, u, as a function of time evaluated on the equator at 110W for Case A. The result for eastward translating fetch (solid line) is compared with that for stationary fetch (dashed line).

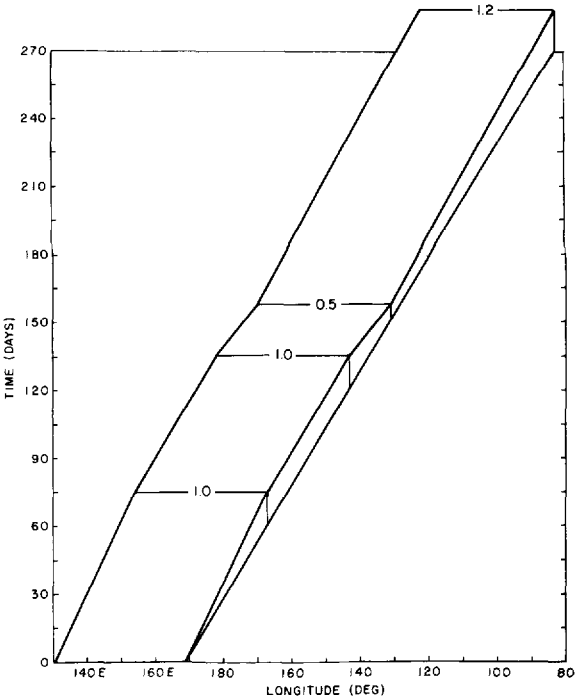

Figure 7. Amplitude modulation of the westerly wind stress anomaly used in Case B as a function of longitude and time. Units are dynes/cm^2.

investigate these behaviors we consider the effect of varying wind stress as the westerly anomaly translates eastward. The westerly wind stress anomaly used is shown as a function of longitude and time in Figure 7. The initial position, fetch, and eastward translation speed are the same as in Case A. The amplitude increases over two months from 0 to 1.0 dynes/cm^2. The amplitude remains constant for two additional months and then decreases to a minimum of 0.5 dynes/cm^2 one month later followed by an increase to 1.2 dynes/cm^2 over the subsequent four month period. Analytically, the forcing function is given by:

$$\begin{aligned}\tau(x, y, t) = \gamma e^{-y^2/2} &\{H(x - \alpha t) - H(x - L - \alpha t)\} \\ &\cdot \left\{\frac{tH(t)}{T_0} - \frac{(t - T_0)H(t - T_0)}{T_0}\right. \\ &- S_1 \frac{(t - T_1)H(t - T_1)}{T_1} \\ &\left. + S_2 \frac{(t - T_2)H(t - T_2)}{T_2}\right\} \end{aligned} \tag{10}$$

where S_1, S_2, T_0, T_1 and T_2 set the amplitude and rate of change of the anomaly. We proceed in the same manner as in Case A except here the interior solutions and their subsequent boundary reflections consist of four parts, the initial increase, the period of constant stress, the decrease, and the final increase. The interior Kelvin wave solution is:

$$\begin{aligned} u_k(x, y, t) = h_k(x, y, t) = &\frac{\gamma\pi^{1/4}}{4T_0(1-\alpha)^2}\psi_0(y) \\ &\cdot \{(x-\alpha t)(t(2-\alpha)-x)H(x-\alpha t) \\ &-(x-L-\alpha t)(t(2-\alpha)-x-L)H(x-L-\alpha t) \\ &+(x-t)^2H(x-t)-(x-L-t)^2H(x-L-t)\} \\ &-F_k(T_0)-S_1F_k(T_1)+S_2F_k(T_2) \end{aligned} \tag{11}$$

where

$$\begin{aligned} F_k(T_m) = \gamma\pi^{1/4}\psi_0(y)\Bigg[&\left(\frac{t}{T_m}-1\right)\{(x-\alpha t)H(x-\alpha t) \\ &-(x-L-\alpha t)H(x-L-\alpha t)\}/2(1-\alpha) \\ &+\{(x-L-\alpha t)^2H(x-L-\alpha t) \\ &-(x-\alpha t)^2H(x-\alpha t) \\ &+(x-t+(1-\alpha)T_m)^2H(x-t+(1-\alpha)T_m) \\ &-(x-t+(1-\alpha)T_m-L)^2H(x-t \\ &+(1-\alpha)T_m-L)\}/4T_m(1-\alpha)^2\Bigg] \end{aligned}$$

and $m = 0, 1, 2$. The interior Rossby wave solution is:

$$\begin{aligned} \begin{bmatrix} u_R(x, y, t) \\ h_R(x, y, t) \end{bmatrix} = &\Bigg[-\frac{\gamma\pi^{1/4}}{4\sqrt{2}\,T_0\,(\alpha+1/3)^2} \\ &\cdot \{-(x-\alpha t)(x+t(\alpha+2/3))H(x-\alpha t) \\ &+(x-L-\alpha t)(x+t(\alpha+2/3))H(x-\mathrm{L}-\alpha t) \\ &+(x+t/3)^2H(x+t/3)-(x-L+t/3)^2H(x-L+t/3)\} \\ &-F_R(T_0)-S_1F_R(T_1)+S_2F_R(T_2)\Bigg] \\ &\cdot \begin{bmatrix} \dfrac{-2\sqrt{2}}{3}\psi_0(y)+\dfrac{2}{3}\psi_2(y) \\ \dfrac{2\sqrt{2}}{3}\psi_0(y)+\dfrac{2}{3}\psi_2(y) \end{bmatrix}. \end{aligned} \tag{12}$$

where

$$
\begin{aligned}
F_R(T_m) = \frac{\gamma\pi^{1/4}}{\sqrt{2}}\Bigg[&\left(\frac{t}{T_m} - 1\right)\{-(x - \alpha t)H(x - \alpha t) \\
&+ (x - L - \alpha t)H(x - L - \alpha t)\}/2(\alpha + 1/3) \\
&+ \Bigg\{-(x - \alpha t)^2 H(x - \alpha t) + (x - L - \alpha t)^2 H(x - L - \alpha t) \\
&+ \left(x + \frac{t}{3} - \left(\alpha + \frac{1}{3}\right)T_m\right)^2 H\left(x + \frac{t}{3} - \left(\alpha + \frac{1}{3}\right)T_m\right) \\
&- \left(x + \frac{t}{3} - \left(\alpha + \frac{1}{3}\right)T_m - L\right)^2 H\left(x + \frac{t}{3}\right. \\
&\left.- \left(\alpha + \frac{1}{3}\right)T_m - L\right)\Bigg\}\Big/4T_m(\alpha + 1/3)^2\Bigg]
\end{aligned}
$$

and $m = 0, 1, 2$. Summing these interior responses with their meridional boundary reflections as in Case A yields the total long wave solution complete through the fifth mode reflected Rossby waves. These are shown on the equator as a function of longitude and time for the upper layer thickness and zonal velocity component perturbation respectively in Figures 8 and 9. Of particular interest in Figure 8, the upper layer thickness perturbation, relative to the Case A counterpart in Figure 3 are: (1) the increase and subsequent decrease in downwelling on the eastern side of the domain prior to the arrival of the wind stress anomaly and (2) the second downwelling peak observed at the eastern boundary toward the end of the calculation.

Figure 10 shows a time slice of the upper layer thickness perturbation at 110W. Note the similarity in shape between it and the temperature variability at the 100 m level during the 1982/83 El Nino event shown in Figure 2. Downwelling proceeds in two phases, first a rapid portion for around two months and then a slower portion for another two months. After reaching a peak the downwelling very rapidly diminishes. In our solution, the first portion corresponds to both the interior downwelling Kelvin wave generated as the amplitude of the wind stress anomaly grows along with the upwelling Kelvin wave reflected from the western boundary. The rate of downwelling decreases as the wind stress reaches a constant and the peak downwelling is attained after passage of the first reflected Rossby mode. The rapid subsidence of downwelling after the peak is primarily associated with the decrease in the amplitude of the westerly wind stress anomaly. This latter feature is distinctly different from Case A. The leveling off around day 180 is mainly a consequence of increasing wind stress with a lesser contribution from the third Rossby mode reflection. The upwelling beyond day 210 results from direct wind forcing since the anomaly has reached 110W, again an artificial result.

The dashed line in Figure 10 shows the response obtained for the variable amplitude

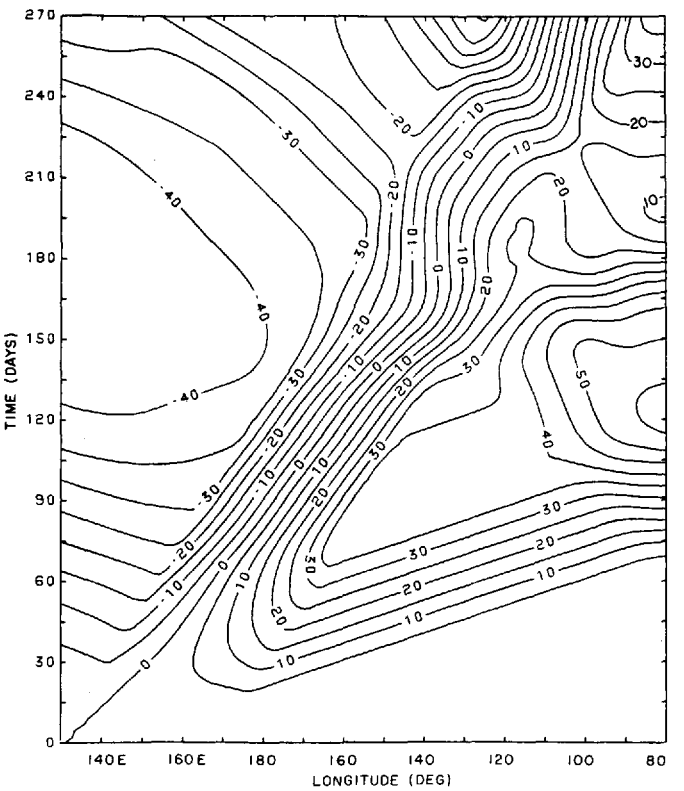

Figure 8. Upper layer thickness perturbation, h, evaluated on the equator as a function of longitude and time for the amplitude modulated westerly wind stress anomaly given in Figure 7 and Eq. 10. The constant fetch and eastward translation speed are again 40° and 50 cm/sec respectively and the reduced gravity wave phase speed, $(g'H_0)^{1/2}$, is 250 cm/sec. The contour interval = 5 m.

Case B when the fetch is kept stationary to the west of the dateline. The efficacy of eastward translation in intensifying the downwelling response is as clearly evident here as in Figure 5.

A time slice of the zonal velocity component at 110W is shown in Figure 11. Its sinusoidal character agrees very well with that observed in Figure 2. Eastward acceleration accompanies the interior downwelling Kelvin wave response. This is slowed by the western boundary reflected Kelvin wave followed by a westward acceleration brought on by the first mode Rossby wave reflection of the interior downwelling Kelvin wave. Figure 11 is a smoothed and phase shifted version of Figure 6 (Case A). Both of these differences are due to the initial linear buildup of the westerly wind anomaly as opposed to an instantaneous onset. The decrease in wind stress also adds to the westward acceleration of Case B but the principal contributor is still the reflected first mode Rossby wave as in Case A.

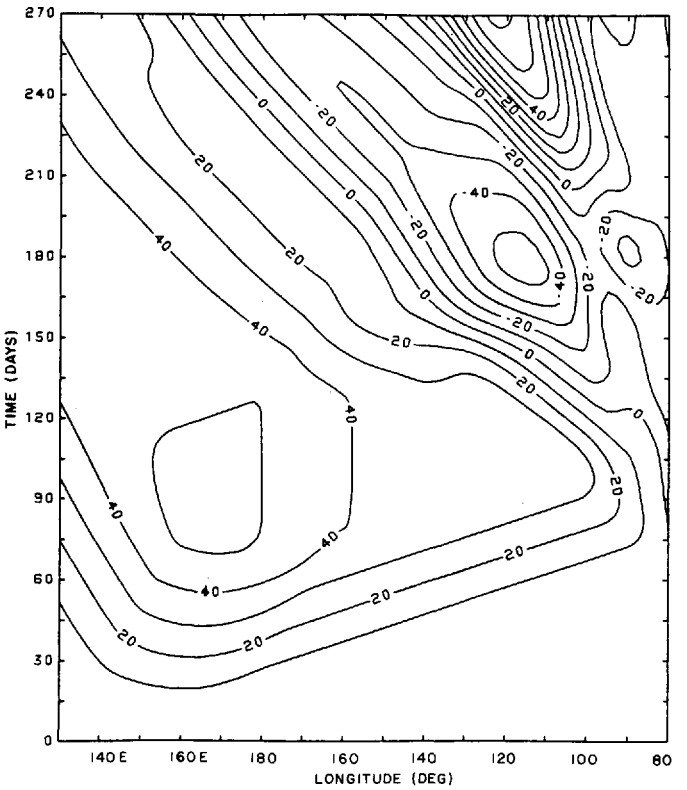

Figure 9. Upper layer zonal velocity component perturbation, u, evaluated on the equator as a function of longitude and time for the amplitude modulated westerly wind stress anomaly given in Figure 7 and Eq. 10. The constant fetch and eastward translation speed are again 40° and 50 cm/sec respectively and the reduced gravity wave phase speed, $(g'H_0)^{1/2}$, is 250 cm/sec. The contour interval = 10 cm/sec.

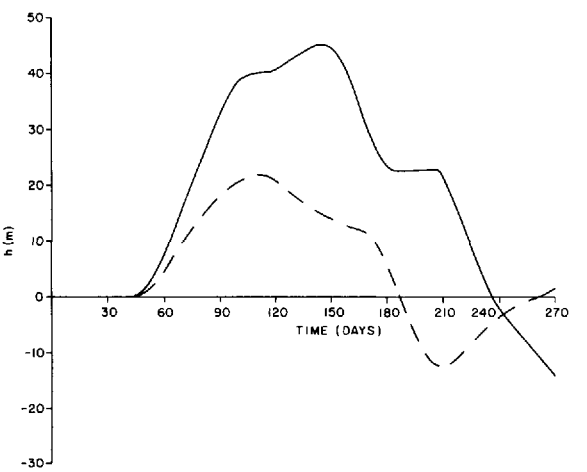

Figure 10. Upper layer thickness perturbation h, as a function of time evaluated on the equator at 110W for Case B. The result for eastward translating fetch (solid line) is compared with that for stationary fetch (dashed line).

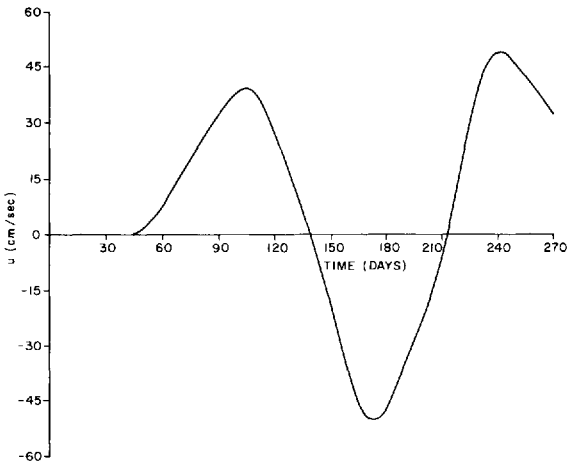

Figure 11. Upper layer zonal velocity component perturbation, u, as a function of time evaluated on the equator at 110W for the eastward translating westerly wind stress anomaly of Case B.

5. Discussion

We set forth to investigate the effects of certain aspects of the wind stress anomaly observed during the 1982/83 El Nino event upon the Pacific Ocean's response. The fact that the westerly wind anomaly moved eastward across the ocean as opposed to remaining stationary to the west of the dateline was shown to result in much larger and longer lived downwelling for the same wind stress fetch and magnitude. The approximate factor of two increase in downwelling and duration shown in either of our Figures 5 or 9 agrees very well with the comparisons made between the 1982/83 event and the composite El Nino SST indices shown by Gill and Rasmusson (1983) or Arkin *et al.* (1983).

Movement alone was not sufficient to account for other interesting features of the 1982/83 event. In order to arrive at the general shape and duration of the downwelling observed at 110W it was necessary to vary the amplitude of the westerly wind stress anomaly as it moved across the Pacific Ocean in accordance with Figure 2. For example, constant wind stress anomaly would not have reduced the downwelling and SST anomaly observed at 110W (Figs. 1 and 2) after Dec. 1982, nor would it have separated the timing of the maximum downwelling peak from the maximum westward current (Fig. 2). More importantly, varying the amplitude resulted in the second downwelling peak observed off the South American coast.

Along with the decrease in westerly wind anomaly amplitude, Figure 1 shows a simultaneous appearance of an easterly anomaly which remains stationary west of 160E with roughly half the speed or one quarter the stress as the westerly anomaly. To consider the effects of this we calculated the response to an easterly stress anomaly

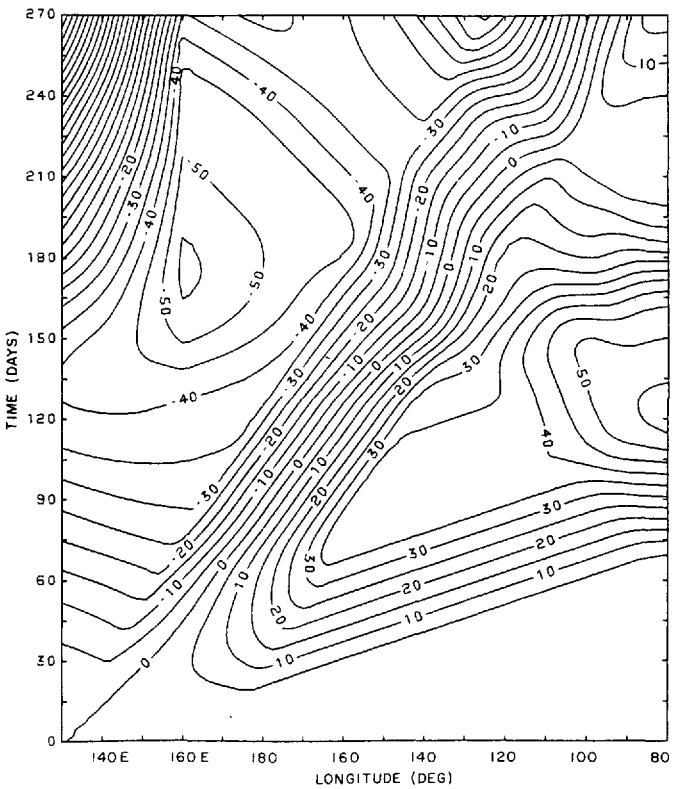

Figure 12. Upper layer thickness perturbation h, evaluated on the equator as a function of longitude and time for the sum of the responses due to the eastward translating westerly wind stress anomaly of Case B and a stationary easterly wind stress anomaly with amplitude 0.25 dynes/cm^2 switched on at day 120 between 130E and 160E. The contour interval = 5 m.

stationary between the western boundary at 130E and 160E which grows to 0.25 dynes/cm^2 over 0.5 months and remains constant thereafter. This solution was then added to Case B and the total results are shown in Figures 12 and 13 for upper layer thickness and zonal velocity component perturbations respectively, both as functions of longitude and time. Figures 12 and 13 are identical to Figures 9 and 10 prior to day 120 when the easterly anomaly was switched on. Several points are notable following day 120. Immediately upon switching on the easterlies the thermocline downwells in the western Pacific. This results in the rapid switch off of the upwelling between 140E and 160E as shown by Rebert *et al.* (1983). Without easterlies the upwelled thermocline would have remained fairly steady for several months. An effect at the South American coast is to further upwell the thermocline after the first downwelling peak which serves to accentuate the second peak to follow. An important effect also occurs at 110W as shown in the upper layer thickness perturbation time slice of Figure 14.

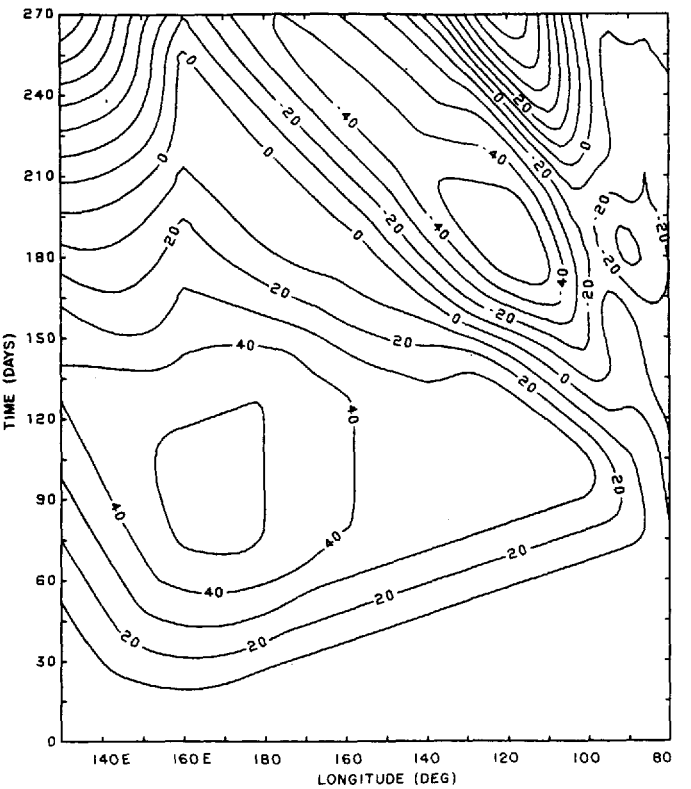

Figure 13. Upper layer zonal velocity component perturbation, u, evaluated on the equator as a function of longitude and time for the sum of the responses due to the eastward translating westerly wind stress anomaly of Case B and a stationary easterly wind stress anomaly with amplitude 0.25 dynes/cm^2 switched on at day 120 between 130E and 160E. The contour interval = 10 cm/sec.

The easterly anomaly provides the additional upwelling necessary to bring the thermocline closer to its normal position after the December downwelling peak (compare Fig. 14 with Figs. 10 and 2). We no longer depend upon the artificial arrival of the westerly wind anomaly at 110W to accomplish this adjustment. Unlike the upper layer thickness, the effect of the easterly anomaly on the zonal velocity component is inconsequential as shown in Figure 15.

One further characteristic of the westerly wind anomaly which we have not considered is the expansion of the fetch westward during the second buildup phase. Since the downwelling associated with the forced interior Kelvin wave is directly proportional to the fetch, increased fetch would correspond to increased downwelling at the coast at the same time that the second peak is forming. Consequently the effect of increased fetch is to amplify the second downwelling peak at the coast.

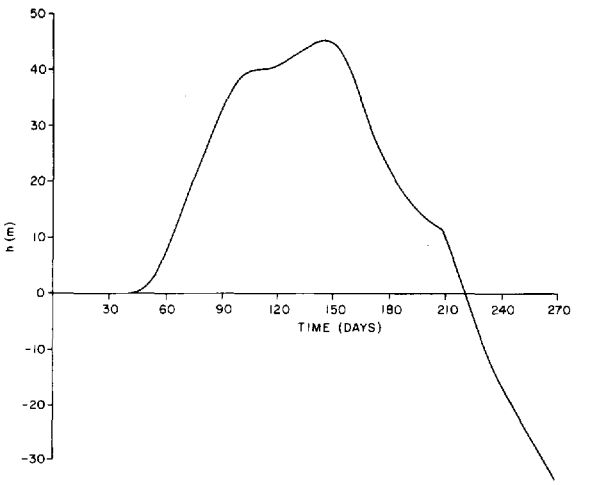

Figure 14. Upper layer thickness perturbation, h, as a function of time evaluated on the equator at 110W for the sum of the responses due to the eastward translating westerly wind stress anomaly with amplitude 0.25 dynes/cm^2 switched on at day 120 between 130E and 160E.

6. Summary and conclusions

The 1982/83 El Nino—Southern Oscillation event in the equatorial Pacific Ocean was the largest one ever documented (Rasmusson and Wallace, 1983). Certain distinctions between the ocean's response to the 1982/83 event and the composite event described by Rasmusson and Carpenter (1982) formed the basis of the present study. We were particularly interested in the relative magnitude and duration of the oceanic downwelling response to the anomalous zonal wind field observed during the event and the double peaked nature of the downwelling.

To investigate whether certain details of the observed wind anomaly field could produce the features of interest, we forced an adiabatic reduced gravity model with different zonal wind anomalies embracing these details. Analytical interior solutions were calculated using the techniques of Cane and Sarachik (1976) and boundary reflections were added using the techniques of Moore and Philander (1977) and Cane and Sarachik (1977). Two principal cases were considered. Case A compared the oceanic response to a westerly wind anomaly of constant amplitude and fetch translating eastward across the basin with a similar anomaly which remained stationary west of the dateline. The eastward translating anomaly produced a larger (by a factor of two) and longer lived downwelling response than the stationary anomaly. Case B investigated the effects of varying the anomaly's amplitude as it traversed the basin. This produced the general shape and duration of the downwelling observed at 110W and the double peaked behavior at the South American coast. We then added an easterly anomaly as appeared to the west of the dateline midway

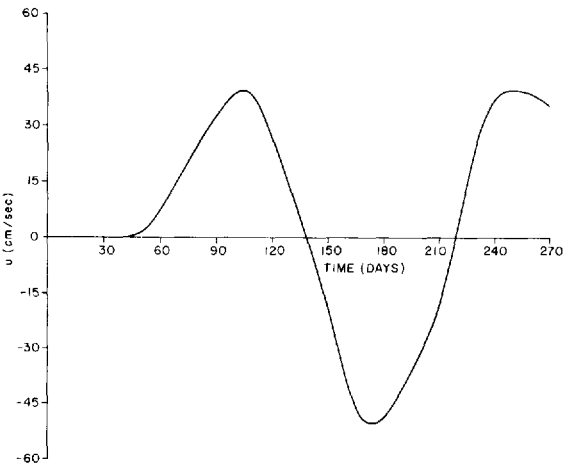

Figure 15. Upper layer zonal velocity component perturbation, u, as a function of time evaluated on the equator at 110W for the sum of the responses due to the eastward translating westerly wind stress anomaly with amplitude 0.25 dynes/cm^2 switched on at day 120 between 130E and 160E. The contour interval = 10 cm/sec.

through the 1982/83 event and discussed its role. Finally, we discussed enhancement of the double peaked coastal response by an increase in the fetch of the westerly anomaly toward the latter stages of the event.

We conclude that the eastward translation of the westerly wind anomaly during the 1982/83 El Nino—Southern Oscillation event was responsible for the relative intensity and duration of the downwelling while the amplitude modulation of the anomaly was primarily responsible for the double peak. What caused the amplitude and fetch modulation remains a particularly important topic for coupled oceanic-atmospheric models. For example, the initial phase of the westerly wind anomaly buildup which occurred for around 4 months resulted in the large scale SST anomaly covering the eastern half of the equatorial Pacific. Was the subsequent increase in the amplitude and fetch of the westerly wind anomaly which in turn caused the second and larger SST peak at the coast the result of positive feedback from the ocean to the atmosphere?

Acknowledgments. This work was supported by both a National Science Foundation grant number OCE-8211848 and a U.S. Dept. of Commerce, NOAA-ERL, contract number NA83RAC00021. Consideration of the easterly wind stress anomaly in Section 5 was at the suggestion of Dr. E. Sarachik. The timely appearance of data in the Tropical Ocean-Atmospheric Newsletter, D. Halpern, ed., was instrumental in stimulating interest for this study.

REFERENCES

Arkin, P. A., J. D. Kopman and R. W. Reynolds. 1983. 1982–1983 El Nino/Southern Oscillation event quick look atlas. NOAA/National Weather Service, National Meteorological Center, Climate Analysis Center, Washington, D.C. 20233 (unpublished manual).

Busalacchi, A. T. and J. J. O'Brien. 1981. Interannual variability of the equatorial Pacific in the 1960's. J. Geophys. Res, *86,* 10901–10907.

Busalacchi, A. T., K. Takeuchi and J. J. O'Brien. 1983. Interannual variability of the equatorial Pacific—revisited. J. Geophys. Res., *88,* 7551–7562.

Cane, M. and E. S. Sarachik. 1976. Forced baroclinic ocean motions. I. The linear equatorial unbounded case. J. Mar. Res., *34,* 629–665.

—— 1977. Forced baroclinic ocean motions: II. The linear equatorial bounded case. J. Mar. Res., *35,* 395–432.

Gill, A. E. and E. M. Rasmusson. 1983. The 1982/3 climate anomaly in the equatorial Pacific. Nature, *306,* 229–234.

Halpern, D. 1983. Variability of the Cromwell Current at 110W before and during the 1982–83 warm event. Tropical Ocean-Atmospheric Newsletter, *21,* 31–34.

Horel, J. D. and J. M. Wallace. 1981. Planetary-scale atmospheric phenomena associated with the Southern Oscillation. Mon. Wea. Rev., *109,* 813–829.

Hurlburt, H. E., J. C. Kindle and J. J. O'Brien. 1976. A numerical simulation of the onset of El Nino. J. Phys. Oceanogr., *6,* 621–631.

Matsuno, T. 1966. Quasi-geostrophic motions in the equatorial area. J. Met. Soc. Japan, *44,* 24–43.

McCreary, J. P. 1976. Eastern tropical ocean response to changing wind systems: with applications to El Nino. J. Phys. Oceanogr., *6,* 632–645.

Moore, D. W. and S. G. H. Philander. 1977. Modelling of the tropical oceanic circulation, *in* The Sea, *6,* E. Goldberg *et al.,* eds., Wiley-Interscience, NY, 319–361.

Philander, S. G. H. 1981. The response of equatorial oceans to a relaxation of the trade winds. J. Phys. Oceanogr., *11,* 176–189.

—— 1983. El Nino Southern Oscillation phenomena. Nature, *302,* 245–301.

Philander, S. G. H., T. Yamagata and R. C. Pacanowski. 1984. Unstable air-sea interaction in the tropics. J. Atm. Sci., *41,* 604–613.

Rasmusson, E. M., P. A. Arkin, A. F. Krueger, R. S. Quiroy and R. W. Reynolds. 1983. The equatorial Pacific atmospheric climate during 1982–83. Tropical Ocean-Atmosphere Newsletter, *21,* 2–3.

Rasmusson, E. M. and T. H. Carpenter. 1982. Variations in tropical sea surface temperature and surface wind fields associated with the Southern Oscillation/El Nino. Mon. Wea. Rev., *110,* 354–384.

Rasmusson, E. M. and J. M. Wallace. 1983. Meteorological aspects of the El Nino/Southern Oscillation. Science, *222,* 1195–1202.

Rebert, J., J. Donquy, G. Eldin and A. Morliere. 1983. Thermal fluctuations in the equatorial Pacific in relation to the 1982–1983 warm event. Tropical Ocean-Atmosphere Newsletter, *21,* 7–8.

Weisberg, R. H. and T. Y. Tang. 1983. Equatorial Ocean response to growing and moving wind systems with application to the Atlantic. J. Mar. Res., *41,* 461–486.

Received: *5 December, 1983;* revised: *11 June, 1984.*